Ultrafast Polarized Fluorescence Measurements on Monomeric and Self-Associated Melittin

Anjali Pandit,[*,†] **Olaf F. A. Larsen,**[‡] **Ivo H. M. van Stokkum,**[‡] **Rienk van Grondelle,**[‡]
Ruud Kraayenhof,[†] **and Herbert van Amerongen**[§]

*Department of Structural Biology, Faculty of Earth and Life Sciences, Vrije Universiteit Amsterdam,
De Boelelaan 1087, 1081 HV Amsterdam, The Netherlands, Division of Physics and Astronomy, Faculty of
Sciences, Vrije Universiteit Amsterdam, De Boelelaan 1087, 1081 HV Amsterdam, The Netherlands, and
Laboratory of Biophysics, Department of Agrotechnology and Food Sciences, Dreijenlaan 3,
6703 HA Wageningen, The Netherlands*

The anisotropic and magic-angle fluorescence decay of the single tryptophan (Trp) residue of melittin, a bee venom peptide, was investigated by time-resolved fluorescence anisotropy using a streak camera setup. The peptide was dissolved either in distilled water or in Hepes/NaOH buffer containing low (10 mM) or high (2 M) concentrations of NaCl, the latter resulting in tetramerized melittin. For melittin in distilled water and low NaCl concentration, two anisotropy decay times were found in the order of ~50 and ~800 picoseconds, reflecting local and overall peptide dynamics, respectively, and for tetramerized melittin, two anisotropy decay times of ~200 and ~5500 picoseconds were found. Decay-associated spectra of the isotropic fluorescence decay show three time components in the range of ~20 picoseconds, ~500 picoseconds, and ~3500 picoseconds, respectively. The relative amplitudes of the latter two change upon the self-association of melittin. This change can be explained by the existence of different rotamers of Trp in melittin, of which one is more favored in the melittin tetramer than in the melittin monomer.

1. Introduction

Melittin is the main component of bee venom from the European honeybee (*Apis mellifera*) and contains twenty-six amino acid residues, of which six are positively charged under physiological conditions. In solution melittin can adopt a random coil monomeric form or a tetrameric state composed of four α-helical monomers, depending on the melittin concentration, ionic strength, and pH of the medium.[1–4] Pressure studies reveal that the pressure-dependent self-association of melittin can be explained by hydrophobic interactions.[5] The crystal structure of the aqueous melittin tetramer has been resolved[6] and shows a tetramer consisting of two dimeric units, each composed of two α-helices oriented in an antiparallel fashion. Temperature-dependent NMR studies have shown that upon heating the positions of the melittin monomers inside the tetramer differ from those in the crystal structure[7] and that the hydrophobic residues of melittin in solution are probably more exposed than in the crystal.[8] The symmetry of the tetramer structure suggests that melittin can also form dimers in solution and that self-association into a tetrameric state is a two-step reaction. However, stable melittin dimers have never been identified,[9] and the self-association process is usually described as one process in which four melittin monomers associate toward one tetrameric state. In the presence of membranes melittin also adopts an α-helical conformation, but the exact oligomeric state (monomeric or oligomeric) and orientation (parallel or perpendicular to the membrane) are still under discussion. It is possible that the membrane-association and -insertion processes involve a self-association or self-dissociation step. Therefore, understanding the mechanism of folding and self-association of melittin has importance for understanding its physiological function as a toxic agent.

The single Trp residue in melittin (Trp19) has often been used as an intrinsic fluorescence probe to monitor the folding and tetramerization of melittin by CD, steady-state fluorescence, and time-resolved fluorescence polarization experiments.[1–4,8,9,10] The self-association process of melittin is accompanied by a blue shift of the Trp fluorescence maximum due to shielding of the Trp residues in a hydrophobic pocket and can be observed by steady-state fluorescence measurements. Time-resolved magic-angle fluorescence and anisotropy measurements provide information about the Trp environment and the mobility of the protein.

A complicating factor in the latter experiments is the heterogeneity in the fluorescence decay of Trp. Trp possesses two lowest excited states, termed ^1L_a and ^1L_b, which lie relatively close to each other. When excited at 280 nm, excitation to both states will occur and interconversion between the ^1L_a and ^1L_b states takes place within picoseconds.[11] For ground state conformers, two classes of rotameric states can be distinguished: rotation of the indole ring around the $C_\alpha-C_\beta$ bond (χ_1), giving three rotamers called g⁻, t, and g⁺, or around the $C_\beta-C_\gamma$ bond (χ_2), giving two rotamers (see Figure 1). Molecular dynamic simulations of Engh et al. suggest that the χ_1 rotamers equilibrated faster than the fluorescence lifetime, whereas the χ_2 rotamers would interconvert on the fluorescence time scale.[12] However, later simulation studies suggest that the fluorescence-decay heterogeneity originates from slow interconversion of the χ_1 rotamers, the χ_2 rotamers interconverting too rapidly to have an effect on the time scale of fluorescence,[13] and that it depends on the treatment of the hydrogen atoms in

* Corresponding author. Fax +31-20-4447999. Telephone +31-20-4447166. E-mail pandit@bio.vu.nl
† Department of Structural Biology, Vrije Universiteit Amsterdam.
‡ Division of Physics and Astronomy, Vrije Universiteit Amsterdam.
§ Department of Agrotechnology and Food Sciences.

Ultrafast Polarized Fluorescence of Melittin

J. Phys. Chem. B, Vol. 107, No. 13, 2003 **3087**
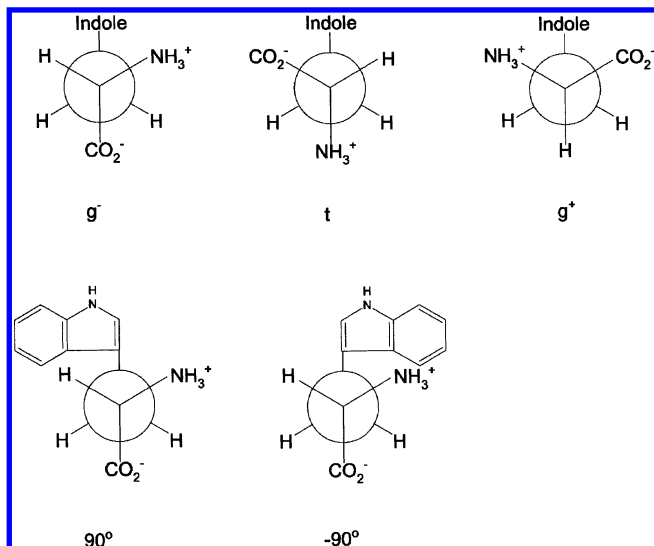
Figure 1. Three rotamers of Trp around the C_α–C_β bond (χ_1), called g^-, t, and g^+, and two rotamers around the C_β–C_γ bond (χ_2).

the simulation.[14] The non-monoexponential decay of Trp fluorescence has often been ascribed to the presence of the above-mentioned rotamers.[15-17] It has been proposed that this effect might also be caused by spectral relaxation.[18,19] Arguments for spectral relaxation are observations of increased fluorescence decay times and emission shift to longer wavelengths with increased excitation wavelengths, and a shift of the emission to shorter wavelengths due to collisional quenching. Furthermore, it has been discussed that for Trp residues in proteins actually the fluorescence of *N*-acetyl-L-tryptophanamide (NATA) is observed, because the amino and carboxyl groups of Trp residues are uncharged due to their participation in the peptide backbone.[19]

When non monoexponential fluorescence decay of Trp in proteins is caused by the presence of rotamers only, the fluorescence exhibits a multiexponential decay, of which the preexponential amplitudes of the fluorescence lifetime components reflect the relative populations of each rotamer. This provides a tool to probe the secondary structure of proteins, as the fractional distribution of the rotamers depends on the main chain conformational constraints.[20,21]

In this work we use time-resolved fluorescence depolarization to examine the self-association process of melittin. The use of a streak camera setup enables us to monitor the fluorescence decay of the complete emission spectrum of the Trp residue over a large time interval ranging from a few picoseconds to a few nanoseconds. Combining this technique with global analysis fitting yields the lifetimes and decay-associated spectra of both short-lived and long-lived fluorescence components. This gives a full picture of the rotational motions of the (complexed) protein and of its Trp residue together with the emission spectra of the supposed rotameric states.

2. Materials and Methods

2.1. Materials. Melittin from bee venom (85% pure by HPLC) was purchased from Sigma-Aldrich Chemie BV (Netherlands) and used without further purification. The melittin concentration was determined from the absorption at 280 nm, using a molar absorption coefficient of 5600 cm^{-1}.

2.2. Steady-State Fluorescence Measurements. Steady-state magic angle fluorescence measurements were performed on an SLM-Aminco AB 2 spectrofluorimeter (Spectronics Instruments, Rochester, NY). For Trp fluorescence experiments the excitation

wavelength was set at 300 nm and the excitation and emission monochromator bandwidths were both set at 4 nm. Because of specific interactions that may occur between charged melittin residues and some buffer salts containing small ions, Hepes was chosen as a suitable buffer.

2.3. Streak Camera Setup. For excitation, pulses of 40 or 125 kHz, centered at 300 nm with a pulse width of ∼100 fs, were produced by the frequence-doubled output of an pptical parametric amplifier (Coherent). The excitation beam was either vertically or horizontally polarized using a Berek polarization compensator, and vertically polarized emission light was selected using a Glan-Thompson polarizer. The emission light was led into a spectrograph (Chromex, Albuquerque, NM) and monitored using a streak-camera system (Hamamatsu) coupled to a CCD camera (Hamamatsu).[22] The fluorescence decay of the complete (polarized) emission spectrum was measured with a time response of ∼4 ps full width at half-maximum over a time regime of 2.2 ns. By using the "backsweep" of the synchroscan system,[23] longer times (up to 10 ns) could also be estimated.

Samples were thermostated at 21 °C using a temperature-controlled cuvette holder. Melittin was dissolved in distilled water, in 10 mM Hepes/NaOH and 10 mM NaCl pH 7.5, or in 100 mM Hepes/NaOH and 2 M NaCl pH 7.5. The optical density was maximal 0.4 at 300 nm and excitation was performed at the very edge of the cuvette to prevent inner filter effects.

2.4. Global Analysis of Time-Resolved Polarized Fluorescence Measurements. Data were analyzed using a parallel global analysis fitting procedure.[24] Parallel and perpendicular polarized time-dependent fluorescence spectra were fitted simultaneously using

$$\begin{bmatrix} I_{VV}(t) \\ I_{HV}(t) \end{bmatrix} = \begin{bmatrix} I_{MA}(1 + 2r(t)) \\ I_{MA}(1 - r(t)) \end{bmatrix} \otimes I(t) \qquad (1)$$

in which $I_{VV}(t)$ and $I_{HV}(t)$ are the parallel and perpendicular polarized emission intensities, $I_{MA}(t)$ is the magic-angle fluorescence, r is the anisotropy, and $I(t)$ is the instrument response. The magic-angle fluorescence $I_{MA}(t)$ was fitted with three decay components according to

$$I_{MA}(t) = \sum_{i=1}^{3} a_i(\lambda)\, e^{-t/\tau_i} \qquad (2)$$

in which τ_i are the isotropic fluorescence decay time-constants. To correct for Raman scatter, an instantaneous component $I(t)$ was added, which has a maximum intensity at 330 nm. The anisotropy was fitted with a linear combination of two components according to

$$r(t) = \sum_{j=1}^{2} r_j\, e^{-t/\phi_j} \qquad (3)$$

in which ϕ_j are the rotational correlation time constants. Additional fitting components did not lead to a significant improvement of the fits.

3. Results

We prepared samples of melittin dissolved in three different media: (1) bidistilled water, (2) buffer containing 10 mM Hepes and 10 mM NaCl, and (3) buffer containing 100 mM Hepes and 2M NaCl. Steady-state fluorescence spectra of the samples (1) and (2) both had Trp emission maxima at 345 nm, and sample (3) had a Trp emission maximum at 330 nm (not shown).
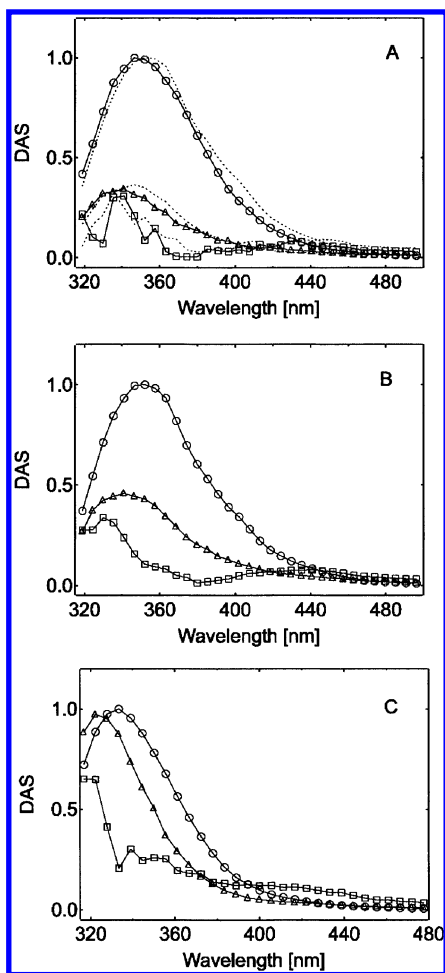
Figure 2. DAS of melittin dissolved in distilled water (A), in 10 mM Hepes + 10 mM NaCl (B), and in 100 mM Hepes + 2M NaCl (C). The DAS belong to the ∼25 ps decay component (squares), ∼500 ps component (triangles) and ∼3.5 ns component (circles). For comparison, the DAS of free Trp are also drawn in A (dotted spectra). Note that some Raman scatter is still present in the ∼25 ps component, contributing in the region 320−360 nm.

Time-resolved fluorescence spectra of (1), (2), and (3) were analyzed by a nonassociative global-analysis fitting model, assuming that the anisotropy decay can be represented by the sum of two exponential components and assuming that the magic angle fluorescence decay can be represented as a sum of three exponential components (see Materials and Methods). Figure 2 shows the decay-associated spectra (DAS) of sample 1 (2A), sample 2 (2B) and sample 3 (2C). The DAS belong to a very fast component with a fluorescence decay-time in the order of ∼25 picoseconds, followed by two slower components with decay times in the order of ∼500 picoseconds and ∼3.5 nanoseconds, respectively. In Figure 2A, the DAS of Trp is also drawn for comparison (dotted spectra). The latter DAS is obtained from measurements of Larsen et al.[25] Figure 3 shows the fluorescence center-of-gravity as a function of time, plotted for sample 1 and 2 in 3A and plotted for sample 3 in 3B. The DAS belonging to the ∼25 ps component has a very redshifted emission (centered around 420 nm), and therefore the center-of-gravity plots of all three samples show a fast blue shift, followed by a small red shift. The isotropic fluorescence-decay times and the rotational correlation times of the (monomeric or complexed) protein and the isotropic fluorescence decay times are shown in Table 1. In this table also the values obtained for free Trp are displayed for comparison. For monomeric melittin (samples 1 and 2), two rotational correlation times are found in
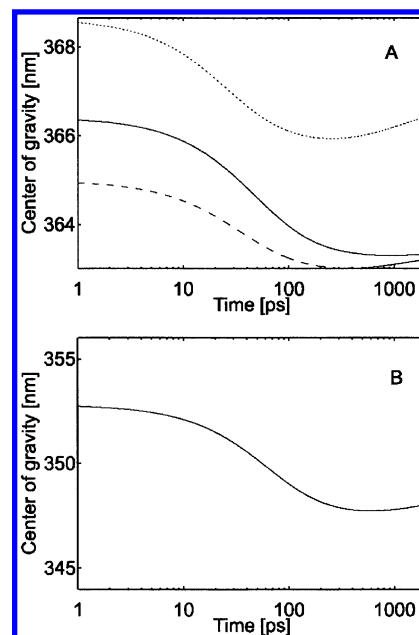
Figure 3. Lin-log plots of the emission center-of-gravities for melittin in distilled water (A, solid line), melittin in 10 mM Hepes + 10 mM NaCl (A, dashed line), and for melittin in 100 mM Hepes + 2M NaCl (B). For comparison, the center-of-gravity of free Trp are also drawn in A (dotted line).

TABLE 1: Magic-Angle and Anisotropic Decay Parameter[s]

sample	τ_i [ps]	a_i	ϕ_i	r_i
MLT in distilled water	3240	0.66	50	0.09
	410	0.21	860	0.20
	25	0.13		
MLT in 10 mM Hepes	3900	0.60	62	0.05
	480	0.25	770	0.17
	20	0.15		
MLT in 100 mM Hepes, 2 M NaCl	3450	0.43	210	0.02
	570	0.33	5450	0.30
	36	0.24		
Trp in 50 mM K phoshate	3800	0.64	44	0.26
	500	0.20		
	13	0.16		

[a] Parameters: τ_i magic-angle decay time constant, a_i magic-angle decay amplitude, ϕ_i anisotropic decay time constant, r_i magic-angle decay amplitude. The errors in the presented values are approximately 10%.

the order of ∼55 picoseconds and ∼800 picoseconds, corresponding to rotation of the Trp residue and of the whole protein, respectively. For tetrameric melittin (sample 3), both rotational correlation times are slower: 210 and 5450 picoseconds, respectively.

In our global-analysis model, the anisotropy at time zero (r_0 = r_1 + r_2) was assumed to be constant over the fluorescence emission range. However, time traces at single emission wavelengths show an emission-dependent time-zero anisotropy, and the sum of r_1 and r_2 actually displays the fitted r_0 averaged over the emission range. This is demonstrated in Figure 4. Figure 4 shows the horizontally and vertically polarized fluorescence decay traces at 365 nm and at 474 nm for tetrameric melittin (sample 3), and the corresponding time-resolved anisotropy r = $(I_{VV} - I_{HV})/(I_{VV} + 2I_{HV})$ (insets). The traces are taken from the raw streak-camera data, of which the time zero was adjusted using a dispersion correction. At 365 nm, r_0 is 0.33 (± 0.02)

Ultrafast Polarized Fluorescence of Melittin

J. Phys. Chem. B, Vol. 107, No. 13, 2003 **3089**
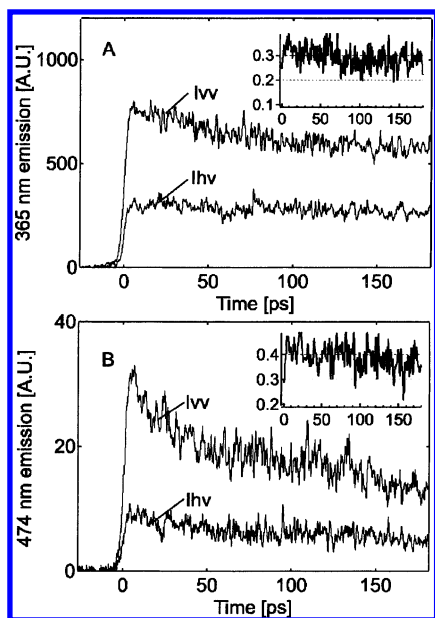
Figure 4. Parallel and perpendicular polarized fluorescence time traces of melittin dissolved in 100 mM Hepes + 2M NaCl (A, 365 nm emission and B, 474 nm emision) with in the insets the anisotropy.

and at 474 nm r_0 is 0.4 ($\pm$ 0.04). The horizontally and vertically polarized fluorescence traces at 474 nm contain a fast (about 20 ps) decay component that is absent at 365 nm. However, this fast decay component is not present in the time-dependent anisotropy trace (see inset Figure 4B). Hence, this fast red fluorescence decay is isotropic and not accompanied by a fast depolarization. Note that at 474 nm emission the anisotropy is as high as 0.4, indicating that no depolarization process has taken place of which fluorescence is emitted at this wavelength.

4. Discussion

4.1. Different Fluorescence Lifetimes Reflect Different Rotameric States Rather than Spectral Relaxation. It has been argued that the non-monoexponential decay of Trp fluorescence in proteins is caused by spectral relaxation rather than by the presence of different rotameric states.[19] However, we believe that in this study the observed non-monoexponential fluorescence decay cannot be ascribed to spectral relaxation. First, the center-of-gravity plots show a fast large blue shift before a small red shift is displayed, instead of a red shift only as expected for spectral relaxation. Second, there seems to be no correlation between the fast depolarization times in the order of 50 picoseconds (displaying the rotational correlation time of the Trp residue) and the observed red shift in the order of 700 picoseconds. Hence, the Trp residue has experienced maximal rotation (under the restrictions caused by its binding to the peptide backbone) before the red shift takes place. It is unreasonable to think that the reorientation of water molecules would occur on a slower time scale (700 ps) than reorientation of the Trp residue (50 ps), which is water exposed in monomeric melittin (samples 1 and 2 contain monomeric melittin, see Results). Third, the DAS of melittin in distilled water are nearly identical to the DAS of free Trp (see Figure 2A). Therefore, it is very unlikely that the fluorescence-decay components of the two samples should be ascribed to different mechanisms, i.e., the presence of different rotamers for isolated Trp and spectral relaxation for Trp in melittin.

As mentioned by Larsen et al.,[25] the fast red decay component can also not be ascribed to fast internal L_a-L_b conversion. This effect takes place on a faster time scale (1.6 picoseconds

according to ref 11), and the relatively low time-zero values we find for the anisotropy (averaged r_0 is 0.2 to 0.3) indicate that this internal conversion, accompanied by nonrotational anisotropic decay, already has taken place within the instrument response time of our measurement.

4.2. Monomeric And Self-Associated Melittin Contain Different Rotameric Distributions of Trp. Because the fastest Trp fluorescence-decay component can be ascribed neither to a spectral relaxation process nor to internal L_a-L_b conversion, it is most likely that this component arises from one of the possible rotameric states of Trp. This fast red decay component was recently also observed for free Trp and for single Trp in another small peptide,[25] but has not been observed before by others. For all samples, this fast red-shifted fluorescence decay component was somewhat slower than for free Trp (20−36 picoseconds compared to 13 picoseconds). This fast component also exists for tetrameric melittin (sample 3), although no fast depolarization takes place (the fastest rotational correlation time being as slow as 210 picoseconds with a small amplitude). This demonstrates that the fast red isotropic fluorescence emission decay is not accompanied by a fluorescence depolarization.

Our global analysis fitting revealed only one nanosecond component for the isotropic fluorescence decay, instead of two that are often found for time-resolved measurements on Trp residues. This does not exclude the presence of a second nanosecond component, but the restricted time range of the streak camera (2.2 ns) is too short to determine.

Next to the fast red fluorescence decay component, the ~700 ps and the ~3.5 ns fluorescence decay component can also result from the existence of two different rotamers of the Trp residues. The ratio of these two components alters upon tetramerization. We calculated this ratio by taking the ratio of the peak amplitudes of the resolved decay-associated spectra. Note that this ratio differs from the ratio of the amplitudes of the DAS presented in Table 1, because the amplitudes reflect the area of the DAS. The ratio of the DAS amplitudes would not reflect the true ratio of the fluorescence contributions: in our analysis fluorescence was only analyzed above 325 nm to avoid the Rayleigh scatter at 300 nm. Although Raman scatter around 330−340 nm appears in the DAS belonging to the fastest time component, it does not influence the DAS of the two slower components. Because the fluorescence shifts to shorter wavelengths upon tetramerization, part of the DAS disappeared from the wavelength window upon tetramerization, especially the DAS of the ~500 ps component. For melittin in distilled water (sample 1), the ratio between the peak amplitudes of the ~500 ps and ~3.5 ns DAS is 1:3. This ratio is also found for free Trp in solution (Figure 2A shows that the DAS peaks of free Trp and sample 1 are nearly the same). Also, the rotational correlation times of free Trp and of the Trp residue in random-coiled melittin (sample 1) are comparable (44 and 50 ps respectively, both with an error of 10%). From this can be concluded that the rotameric conformations present in free Trp are not hindered by interactions with the peptide backbone in melittin in a random-coil conformation. For melittin in 10 mM NaCl buffer (sample 2), the ratio of the ~500 ps and ~3.5 ns DAS is 1:2. Apparently, the distribution between the different rotameric components changes upon changing the solution from pure water to low-ionic-strength buffer, although the steady-state emission spectra remain the same (both samples 1 and 2 have a peak maximum at 350 nm) and the rotational correlation times are in the same range (~50 ps and ~860 ps and ~62 ps and ~770 ps respectively). This could indicate that the melittin monomers start folding into an α-helix upon increasing the ion

concentration, before they start associating. The fact that the overall rotational correlation time constant for sample 2 is somewhat shorter than for sample 1 might be explained by a difference in conformation (from random coiled to α-helical). Tetramerization of the peptide in sample (2) is very unlikely, as this should give an increase of the overall rotation time and a blue shift of the steady-state fluorescence. For completely tetramerized melittin, sample (3), the ratio of the ∼500 ps and ∼3.5 ns DAS is 1:1. Apparently, the ∼500 ps rotameric component is relatively more favored in the tetrameric structure than in monomeric melittin and single Trp. An interesting speculation would be that each melittin tetramer consists of two monomers with Trp residues in the conformation of the ∼500 ps rotamer and two monomers with Trp residues in the conformation of the ∼3.5 ns rotamer.

In the crystal structure of melittin, all Trps are most close to the $\chi_2 = 90°$, $\chi_1 = t$ rotameric conformation. The structure might, however, represent an average of the possible rotameric states. Also, as noted by Kemple et al., the nature of the tetramer itself is solvent- and concentration-dependent, and this could be reflected in the dynamics.[26]

The overall rotation correlation time constants for monomeric melittin are somewhat shorter than reported by others (values are reported ranging from 1200 to 2000 picoseconds[10,26-28]). Upon tetramerization, the overall rotation correlation time constant increases and the fast ∼50 ps rotational correlation time of the Trp residue disappears. Instead, a much slower second rotational correlation time (210 ps) can be extracted, but with a very small amplitude. The small amplitude of the Trp rotational correlation time indicates that the movements of Trp inside the tetramer pocket are severely restricted in spatial amplitude.

References and Notes

(1) Talbot, J. C.; Dufourcq, J.; de Bony, J.; Faucon, J. F.; Lussan, C. *FEBS Lett.* **1979**, *102*, 191−193.

(2) Bello, J.; Bello, H. R.; Granados, E. *Biochemistry* **1982**, *21*, 461−465.

(3) Quay, S. C.; Condie, C. C. *Biochemistry* **1983**, *22*, 695−700.

(4) Goto, Y.; Hagihara, Y. 1992 *Biochemistry* **1992**, *31*, 732−738.

(5) Thompson, R. B.; Lakowicz, J. R. *Biochemistry* **1984**, *23*, 3411−3417.

(6) Terwilliger, T. C.; Eisenberg, D. *J. Biol. Chem.* **1982**, *257*, 6010−6015.

(7) Iwadate, M.; Asakura, T.; Williamson, M. P. *Eur. J. Biochem.* **1998**, *257*, 479−487.

(8) Hagihara, Y.; Oobatake, M.; Goto, Y. *Protein Sci.* **1994**, *3*, 1418−1429.

(9) Schubert, D.; Pappert, G.; Boos, K. *Biophys. J.* **1985**, *48*, 327−329.

(10) Lakowicz, J. R.; Gryczynski, I.; Wiczk, W.; Laczo, G.; Prendergast, F. C.; Johnson, M. L. *Biophys. Chem.* **1990**, *36*, 99−115.

(11) Ruggiero, A. J.; Todd, D. C.; Fleming, G. R. *J. Am. Chem. Soc.* **1990**, *112*, 1003−1014.

(12) Engh, R. A.; Chen, L. X. Q.; Fleming, G. R. *Chem. Phys. Lett.* **1986**, *126*, 365−371.

(13) Hu, Y.; Fleming, G. R. *J. Phys. Chem.* **1991**, *94*, 3857−3866.

(14) Gordon, H. L.; Jarrel, H. C.; Szabo, A. G.; Willis, K. J.; Somorjai, R. L. *J. Phys. Chem.* **1992**, *96*, 1915−1921.

(15) Szabo, A. G.; Rayner, D. M. *J. Am. Chem. Soc.* **1980**, *102*, 554−563.

(16) Petrich, J. W.; Chang, M. C.; McDonald, D. B.; Fleming, G. R. *J. Am. Chem. Soc.* **1982**, *105*, 3824−3832.

(17) Dahms, T. E. S.; Willis, K. J.; Szabo, A. G. *J. Am. Chem. Soc.* **1995**, *117*, 2321−2326.

(18) Ladokhin, A. S. *J. Fluoresc.* **1999**, *9*, 1−9.

(19) Lakowicz, J. R. *Photochem. Photobiol.* **2000**, *72*, 421−437.

(20) Willis, K. J.; Neugebauer, W.; Sikorska, M.; Szabo, A. G. *Biophys. J.* **1994**, *66*, 1623−1630.

(21) Dahms, T. E. S.; Szabo, A. G. *Biophys. J.* **1995**, *69*, 569−576.

(22) Larsen, O. F. A.; van Stokkum, I. H. M.; Gobets, B.; van Grondelle, R.; van Amerongen, H. *Biophys. J.* **2001**, *81*, 1115−1126.

(23) Kleima, F. J.; Hofmann, E.; Gobets, B.; van Stokkum, I. H. M.; van Grondelle, R.; Diederichs, K.; van Amerongen, H. *Biophys. J.* **2000**, *78*, 344−353.

(24) van Stokkum, I. H. M.; Scherer, T.; Brouwer, A. M.; Verhoeven, J. W. *J. Phys. Chem.* **1994**, *98*, 852−866.

(25) Larsen, O. F. A.; van Stokkum, I. H. M.; Pandit, A.; van Grondelle, R.; van Amerongen, H. *J. Phys. Chem. B* **2003**, *107*, 3080.

(26) Kemple, M. D.; Buckley, P.; Yuan, P.; Prendergast, F. G. *Biochemistry* **1997**, *36*, 1678−1688.

(27) Zhu, L.; Prendergast, F. G.; Kemple, M. D. *J. Biomol. NMR* **1998**, *12*, 135−144.

(28) Lakowicz, J. R.; Cherek, H.; Gryczynski, I.; Joshi, N.; Johnson, M. L. *Biophys. J.* **1987**, *51*, 755−768.